World Academy of Science, Engineering and Technology
International Journal of Environmental and Ecological Engineering
Vol:9, No:3, 2015

Analysis of a Coupled Hydro-Sedimentological Numerical Model for the Tombolo of GIENS

Yves Lacroix, Van Van Than, Didier Leandri, Pierre Liardet

***Abstract*—**The western Tombolo of the Giens peninsula in southern France, known as Almanarre beach, is subject to coastal erosion. We are trying to use computer simulation in order to propose solutions to stop this erosion. Our aim was first to determine the main factors for this erosion and successfully apply a coupled hydro-sedimentological numerical model based on observations and measurements that have been performed on the site for decades.

We have gathered all available information and data about waves, winds, currents, tides, bathymetry, coastal line, and sediments concerning the site. These have been divided into two sets: one devoted to calibrating a numerical model using Mike 21 software, the other to serve as a reference in order to numerically compare the present situation to what it could be if we implemented different types of underwater constructions.

This paper presents the first part of the study: selecting and melting different sources into a coherent data basis, identifying the main erosion factors, and calibrating the coupled software model against the selected reference period.

Our results bring calibration of the numerical model with good fitting coefficients. They also show that the winter South-Western storm events conjugated to depressive weather conditions constitute a major factor of erosion, mainly due to wave impact in the northern part of the Almanarre beach. Together, current and wind impact is shown negligible.

***Keywords*—**Almanarre beach, coastal erosion, hydro-sedimentological, numerical model.

I. Introduction

THE tombolo of Giens is located in the town of Hyères (Var). It's a double tombolo. Its geographic coordinates are 43.039615 °N to 43.081654 °N and 6.125244 °E to 6.156763 °E. It is located on the French Mediterranean coast, between the Gulf of Giens and Hyères harbor. This double tombolo has two arrows: the western branch (Almanarre beach) and the eastern branch. The Almanarre beach spans almost 4 km, along the Salt Road, and consists of sand and small pebbles (Fig. 1).

Many studies have been conducted about the Almanarre beach. Starting from the 50s, we mention the work of Blanc [1] from the Naval Station in Endoume, about sedimentological aspects of the area. There are also earlier studies on the genesis and evolution of the tombolo [2]-[4]. Since the 70s, more research has been published about sediment transport [5], [6], geomorphological dynamics [7]-[12].

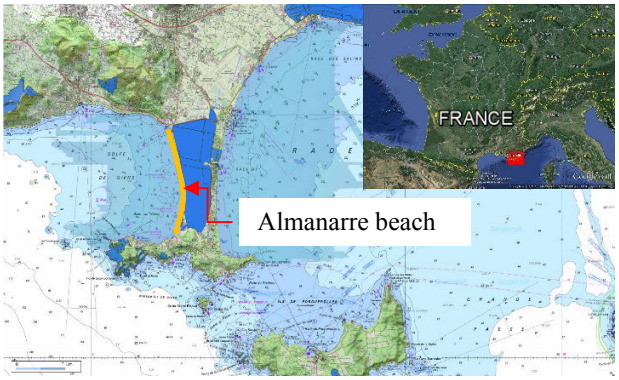

Fig. 1 The Almanarre beach

The Almanarre beach and the side long so called "salt road" have high impact on economical, social and environmental aspects. The area is close to the Marine National Parc of Port Cros, and under supervisor of the Conservatoire du Littoral. Many protection projects have been proposed and some have been implemented, then uninstalled, and no solution yet has been found to stop the erosion process and preserve the area. Each year the salt road is closed during winter time and sand is added to restore the sedimental drift resulting essentially from winter storms.

Numerical models constitute a cheap and non-destructive approach to understand the complex dynamics of the site and propose efficient protection designs. In this paper we present the methodology used to develop a coupled hydro-sedimentological model for the area of the Almanarre beach, using existing available data (most previous studies were funded by public institutions).

II. General Characteristics of the Area

A. Geomorphological Characteristics

We have analyzed the bathymetric data from EGB (European Marine Observation and Data Network Gridded Bathymetry), the Litto3D (Fig. 2) data edited by SHOM (Service Hydrographique et Océanographique de la Marine) and the EOL (Etude et Observation du Littoral) association [10]. The result shows a mean slope of 0.9 to 1% for the area of study, and a distance from the coast to the -30m isobath of

Yves Lacroix is with the UTLN, SEATECH, avenue G. Pompidou, 83162 La Valette du Var, France, and MEMOCS, Università Degli Studi dell'Aquila, Italy (corresponding author to provide phone: 0033(0)683582870; e-mail: yves.lacroix@univ-tln.fr).

Van Van Than is with the AMU, laboratory LATP, Marseille. Research supported by Vietnamese government and WRU, Hanoi, Vietnam (e-mail: thanvanvan@wru.vn).

Didier Léandri is with the AMU, laboratory IGS, Marseille, (e-mail: joba@club-internet.fr)

Pierre Liardet was with the AMU, laboratory LATP, Marseille, France. He left us September 2014.

3.2 km. No underwater reef exists approaching the Almanarre beach.

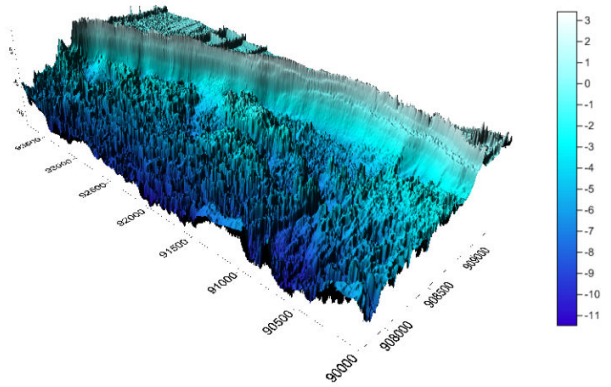

Fig. 2 The high resolution bathymetry (5 m x 5 m) for Almanarre beach from Litto3D

B. Marine Meteorological Conditions

The general climate of the site is maritime Mediterranean climate, characterized by high annual average temperature and sunlight, and particularly mild winters. We identify two prevailing winds regimes [6], [9], [13], [14]. The western regime, dominated by Southwest (230° to 260°) which generates a stir in the Gulf of Giens, and northwest (270° to 300°). The eastern regime (80° to 90°) is "associated with low pressure in the Gulf of Genoa, which is felt strongly throughout the Provençal coast" [7]. Eastern regime represents 30% of the total, and has no influence on the study area which is protected by the tombolo and the peninsula.

C. Hydrodynamic Characteristics

Tide: there is not much data on tides [7], tides in Toulon do not exceed 0.3m.

Swell: it is characterized by strong seasonality based on measurements of waves carried off the buoy network CANDHIS CETMEF (Centre d'Etudes Techniques Maritimes et Fluviales) (08301 buoy and buoy 08302 in Porquerolles): increased heights and periods occurs at the early fall and between September and January. This period presents frequent tempestuous events; February and March record a decline of all the variables; April knows a further increase in relation to the spring equinox storms; between May and August, the variables have the lowest values in relation to the summer anticyclonic regime. The wave rose at the Porquerolles (Fig. 3) show that: the heights of the highest swell is greater than 1.25 m, corresponding to the three dominant directions, northwest, East and South-West; the largest swells (wave height is greater than 4m and period is greater than 10s) correspond mainly to strong northeastern winds (20 m/s) [7].

Agitation depends on swells and sea winds raised by the prevailing offshore winds, and local wind waves related local small fetch winds with waves of 0.5 m on average and short frequencies (2 s to 4 s) [11], [15], [16]. Western and South-Western agitations with medium wave heights are prevalent [16]. The wave heights and angles of incidence may vary depending on the position and power of seagrass (posidonia), the presence of sandstone outcrops [17]. Wave measurements to the coast were performed in Almanarre, November 2000 (Fig. 4), by an Ophiure III wave recorder located 4m deep [8]. Fig. 4 shows that the dominant swells are South-South-West to South-West in the gulf of Giens.

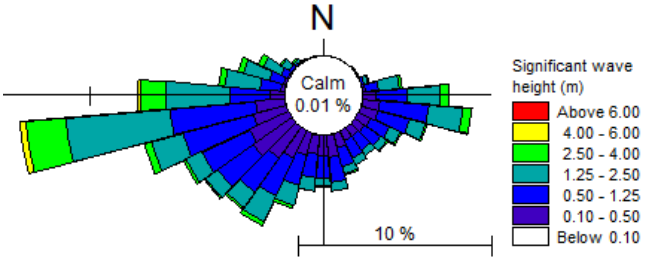

Fig. 3 Wave rose for fourteen years, Porquerolles 1999÷2012

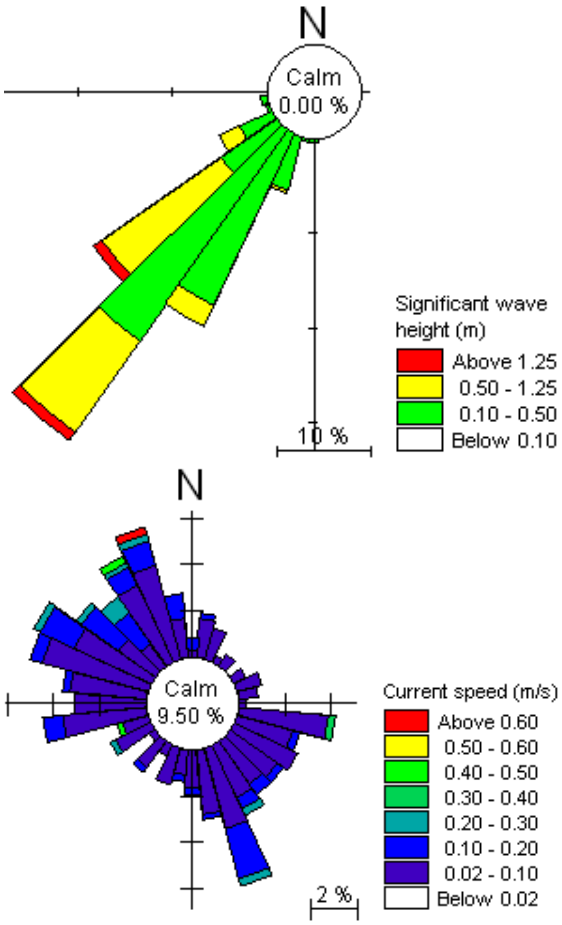

Fig. 4 Wave rose (upper) and current rose (lower) at the Almanarre winter 2000 (2000-10-30 to 2000-11-29)

Currents: longshore currents and rip currents play a key role in the transport of sediments. The speed of the average current is between 3 and 7 cm/s in calm conditions, and rises 15 to 25 cm/s in turmoil ones. The dominant directions on average are east to south and west to north (Fig. 4). During the heavy sea conditions of 6/11/2000, the average speed of the North to West rised from 5 to 25 cm/s in 20 hours [8].

Exceptional events: here is a table of tempest swells in the

gulf of Giens from 1995 to 2008 (see Table I).

TABLE I
TEMPEST SWELLS IN THE GULF OF GIENS FROM 1995 TO 2008

Peak of the storm	$H_{1/3}$	H_{max}	$T_{1/3}$	T_{max}
1995-5-13 5 :00	5.5	9.1	10.4	10.6
1999-12-28 4 :30	5.6	9.2	9.4	10.1
2005-01-21 11 :00	5.6	9	8.4	8.7
2005-02-01 11 :30	6.4	10.2	9.4	9.2
2005-02-13 5 :00	5.6	8.1	8.1	8.9
2007-01-24 0 :30	6.8	12.3	9.8	9.8
2007-02-13 0 :00	5.9	10.4	9	9.4
2007-03-19 17 :00	5.8	9.2	9.2	10.9
2007-05-28 13 :00	5.8	8.8	8.3	8.9
2007-12-10 4 :00	5.5	9.4	7.9	8.8
2008-03-21 3 :00	5.6	9.8	7.6	8
2008-10-30 16 :30	5.8	8.6	8.5	8.7

$H_{1/3}$ = significant wave height; H_{max} = maximum wave height;
$T_{1/3}$ = wave period correspond $H_{1/3}$; T_{max} = pic wave period.

During the strongest storm (24 January 2007) the wind is blowing from southwesterly to northwesterly directions with a wind speed of about 34.21 m/s at the station BAN Hyères.

D. Geomorphologic and Biologic Ground Characteristics

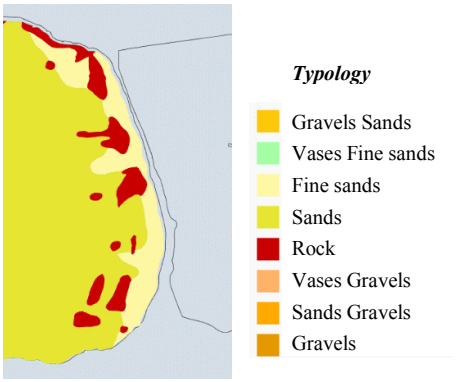

Fig. 5 Sediment map of the gulf of Giens (sources: SHOM and GIS Posidonie)

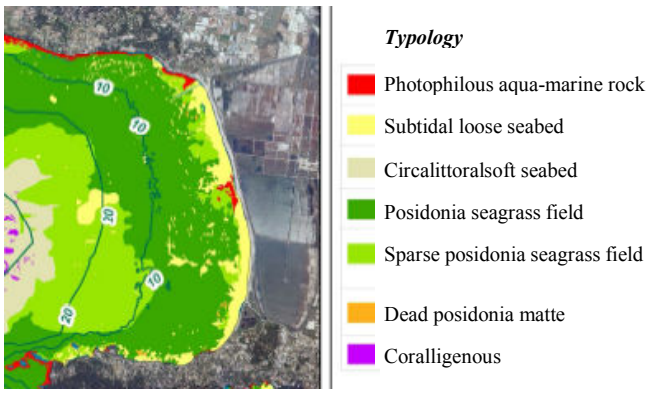

Fig. 6 Biocenosis map of the gulf of Giens (sources: SHOM and GIS Posidonie)

We recovered the mapping of grounds and biological communities on the SHOM site and from the GIS Posidonie (Groupement d'Intérêt Scientifique Posidonie) [18]. Fig. 5 shows that the marine sediments in the area include rock, gravels and fine sand [1], [11].

In the gulf of Giens, the presence of Posidonia had shown in Fig. 6 influence the marine dynamics (wave propagation, wave breaking, currents ...). The Posidonia meadows play an important role in the evolution of morphosedimentary tombolo of Giens. [7]

E. Sea Bed Roughness

In order to take into account posidonia and bed rocks roughness, we need to model them.

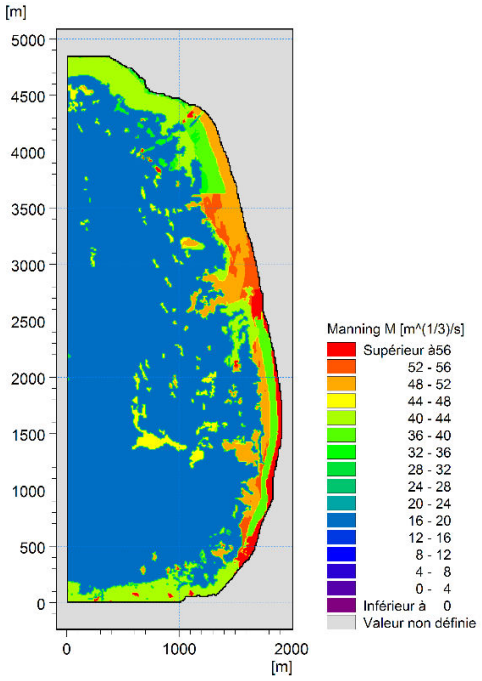

Fig. 7 Different Manning roughness zones

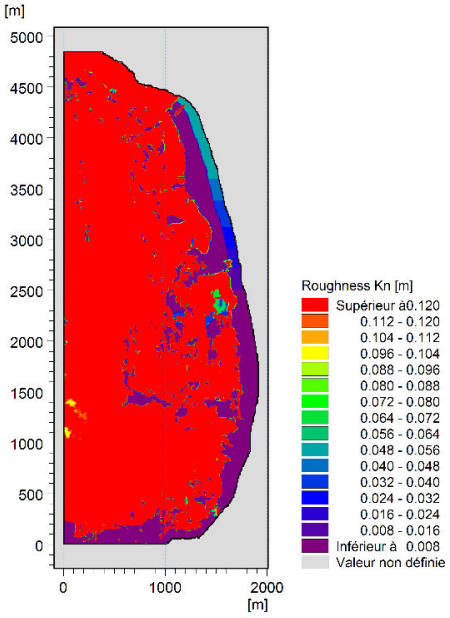

Fig. 8 Different Nikuradse roughness zones

Figs. 7 and 8 show the different roughness classes in the close grid area. Different classes have been identified: posidonia [19], [20], rocks, and sand.

Posidonia roughness depends on square meter beam density, mean leaf width, canopy height and water depth [17], [21].

We model rock bed as sand bed with median diameter D_{50}=20mm. The absence of posidonia generates a higher Manning coefficient (Fig. 7) and a smaller Nikuradse one (Fig. 8).

The Manning number is used as current roughness in the hydrodynamic model (HD). We compute the Spectral Wave Model (SW) with Nikuradse's roughness.

III. Numerical Model

A. Description

The morphodynamical model is based on coupling a wave propagation model (SW) [22], the circulation model (FM) [23], and the sediment transport model (ST) [24] in Mike 21 [25]. The numerical model allows us to illustrate the current due to waves and sediment transport on the coast, as well as the influence on the results of the presence of the posidonia field. The problem is to determine the hydro-sedimentological regime along the Almanarre beach.

1) Regional Scale

The regional scale uses only a SW model.The regional scale spread from Toulon to Cavalaire (40km West-East), uses EGB bathymetry in Lambert 93 projection coordinates and additional data Litto3D (see Fig. 9). The coast line comes from IGN (Institut national de l'Information Géographique et forestière) and SHOM, the wind forced SW model from ECMWF (European Center for Medium range Weather Forecasting). Limiting conditions are swell data collected from the Porquerolles offshore buoy (08301, 08302) (Fig. 9), and from two ANEMOC (Atlas Numérique d'Etats de Mer Océanique et Côtier) spots, MEDIT_2185 and MEDIT_2610.

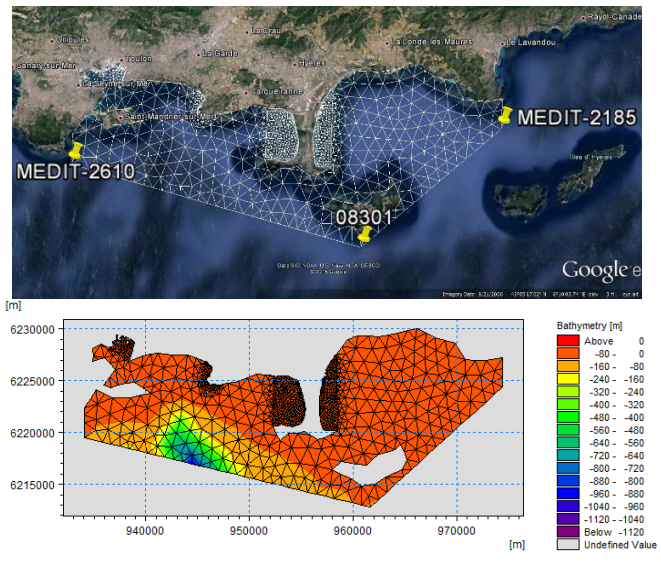

Fig. 9 Computational mesh and regional bathymetry

Mesh and Bathymetry:

The model domain is about 40 km x 10 km with a maximum water depth of approximately 960 m. The overall computational mesh is shown in Fig. 9. The structured mesh includes 1099 nodes and 1811 elements.

A local refinement with higher spatial resolution has been made at the tombolo, Pradet and Toulon harbor. The spatial resolution (mesh size) is smaller than 1.5km (in the gulf of Giens and the gulf of Hyères), and greater than 12m (at the Almanarre beach). The element area ranges from 118 m^2 to 6,5x10^5 m^2.

2) Local Scale

At the local scale in the Fig. 10 we use a coupling of the SW, FM and ST models. The local scale of the model is characterized as follows: the model area extends over Almanarre beach, about 4 km from North to South. The bathymetry results from a combination of the multibeam bathymetry from EOL [10], the Litto3D SHOM assessments, and the EGB, all projected in Lambert 93. The coastline is recovered from IGN and SHOM, the wave model is forced by winds from SYNOP / METAR (Meteorological Airport Report) station of Porquerolles.

The boundary conditions are calculated from the SW model at the regional scale. An average grain size of 0.5 mm is used for sediments. Changes in sea level along the coast are regularly described from Toulon data [6], [7], [9], [11].

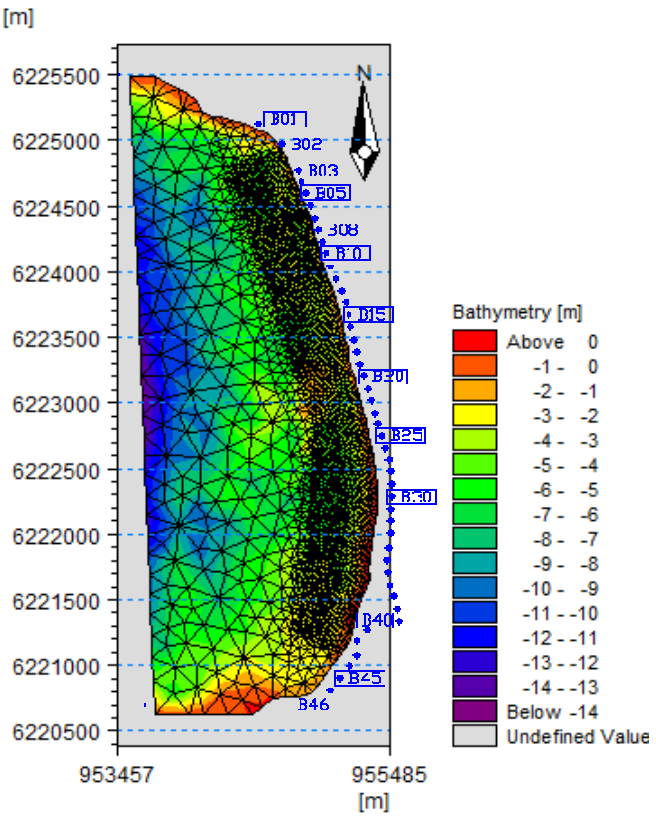

Fig. 10 Local bathymetry and landmarks

Mesh and Bathymetry:

The model domain is about 4 km x 2 km with a maximum water depth of approximately 15 m. The overall computational mesh is shown in Fig. 10. The structured mesh includes 2276 nodes and 4365 elements.

A local refinement with higher spatial resolution has been made at the Almanarre beach. The spatial resolution (mesh size) is smaller than 219m (offshore), and greater than 13m (the surf zone, 400m from the Almanarre beach). The element area ranges from 127m^2 to 4500m^2.

B. Method

The hydro-sedimentological model is two-dimensional horizontal, using a finite volume method. The hydrodynamic system is based on the numerical solution of the two/three-dimensional incompressible Reynolds average Navier-Stokes equations invoking the assumptions of Boussinesq and hydrostatic pressure [26].

The wave model is a model of medium wave propagation includes wave-current interactions. Gravity swell dynamics is described by the transport equation for wave density. There are two methods of simulation of sediment transport in the combined conditions between current and swell: the STP method ("Sediment Transport Program") of DHI (Danish Hydrodynamic Institute) and Bijker's method [24].

We have selected specific short time periods to calibrate the model, adjusting roughness coefficients and sediment dimensions so as to satisfy best fitting criteria for simulation towards the dedicated periods. This rather long part of the work is not presented here as we think it would override the clarity of the exposition. Calibrating data concerned the area of study, Le Pradet (a coastal point 5km from Almanarre) [27], La Capte (on the eastern branch of the tombolo) [28]. We used RMSE, determination coefficient R2 and the Nash-Sutcliffe index, the two last close to one for Nikuradse rugosity, between 0.4 and 0.8 for wave heights [29].

C. Scenarios

We decided to consider six cases of climatic conditions: annual, summer, winter, Mistral wind, western and southwestern storms. The last three incorporate the following data (see Table II).

TABLE II
SCENARIOS FOR NUMERICAL MODEL FOR THE WESTERN TOMBOLO OF GIENS

Scenario	1	2	3
Weather conditions	South-west tempest	Western tempest	Mistral episode
Period of calculus	January	January	January
Wave height, $H_{1/3}$ (m)	6.8	6.8	6.8
Wave period , T (s)	9.8	9.8	9.8
Wave direction, MWD (°)	210	270	270
Wind speed (m/s)	34.21	34.21	34.21
Wind direction (°)	210	270	315

Wave measure at Porquerolles; Wind measure at BAN Hyères.

D. Results

Preliminary hydro-sedimentological simulations for particular periods enabled to define spatio-temporal differences and divide the area into hydro-sedimentological cells. However, details of these results will not be presented in this article. Here we outline the main results.

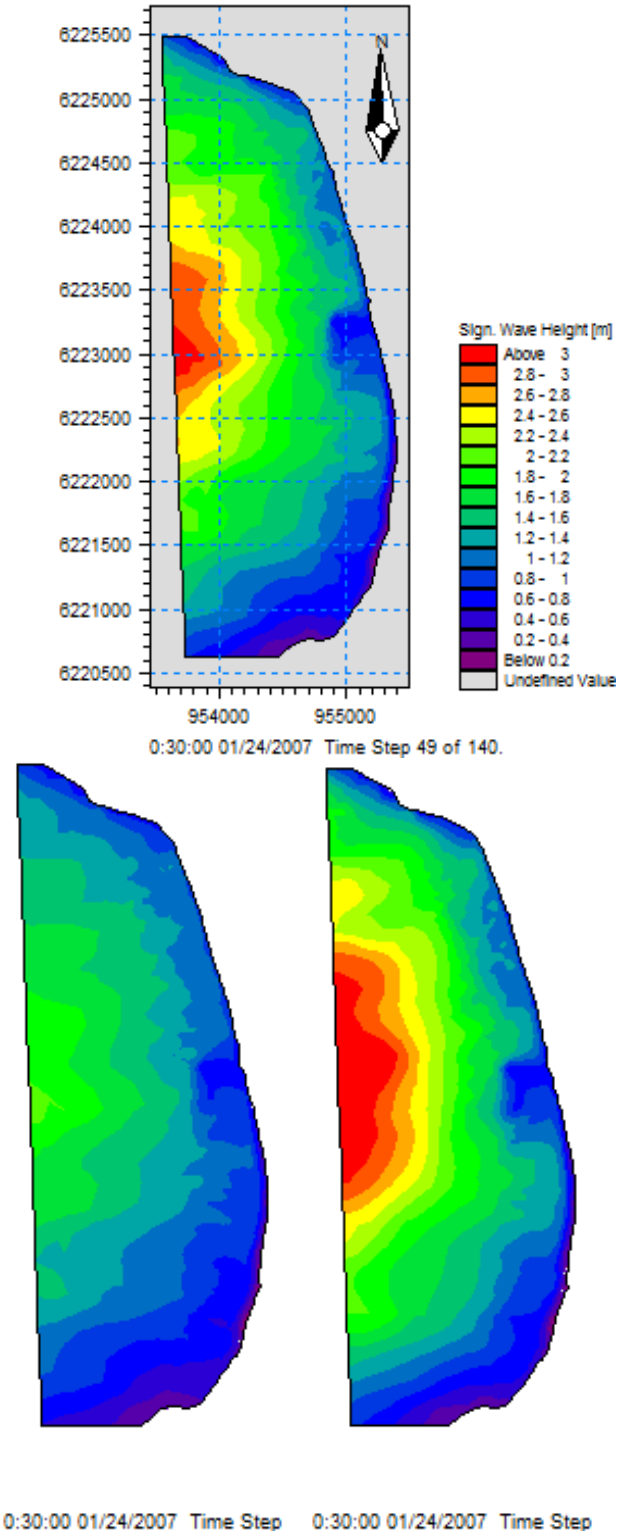

Fig. 11 Maps of the significant wave height (same color palette) at the peak of the western storm (upper), Mistral storm (lower, left), and southwestern storms (lower, right)

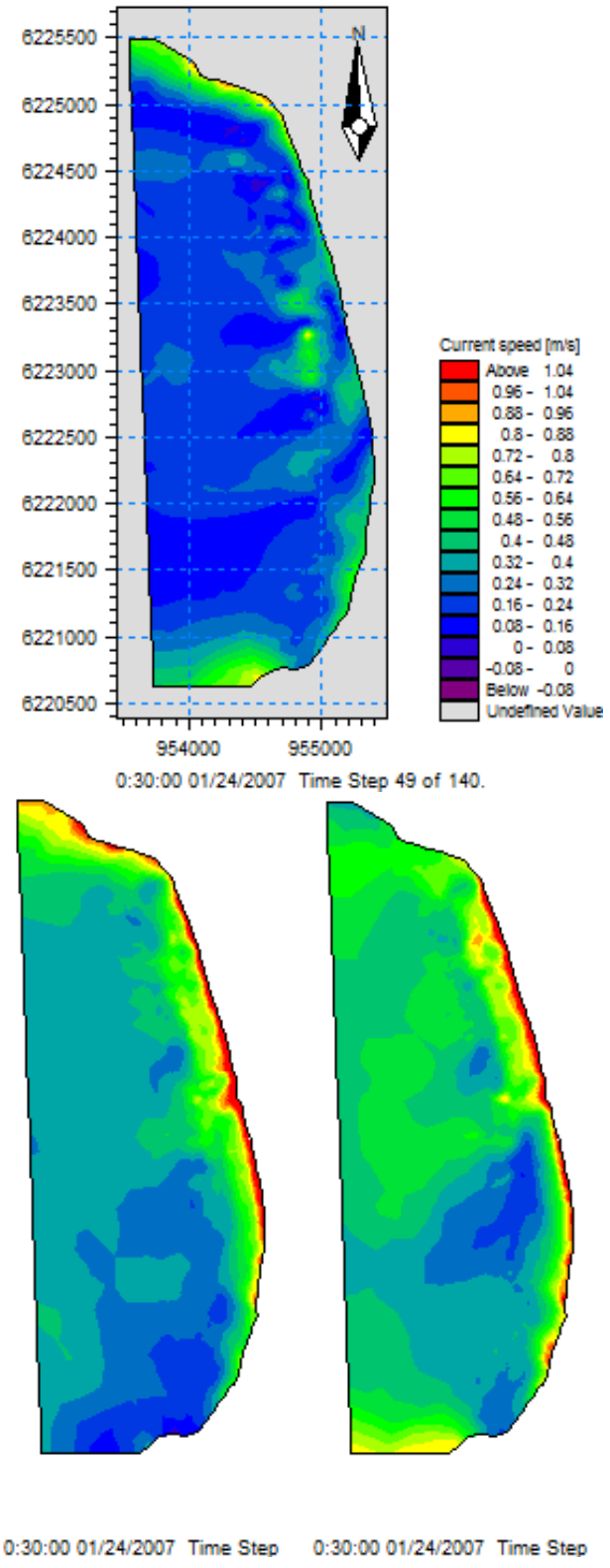

Fig. 12 Maps of the current (same color palette) at the peak of the western storm (upper), Mistral storm (lower, left), and southwestern storms (lower, right)

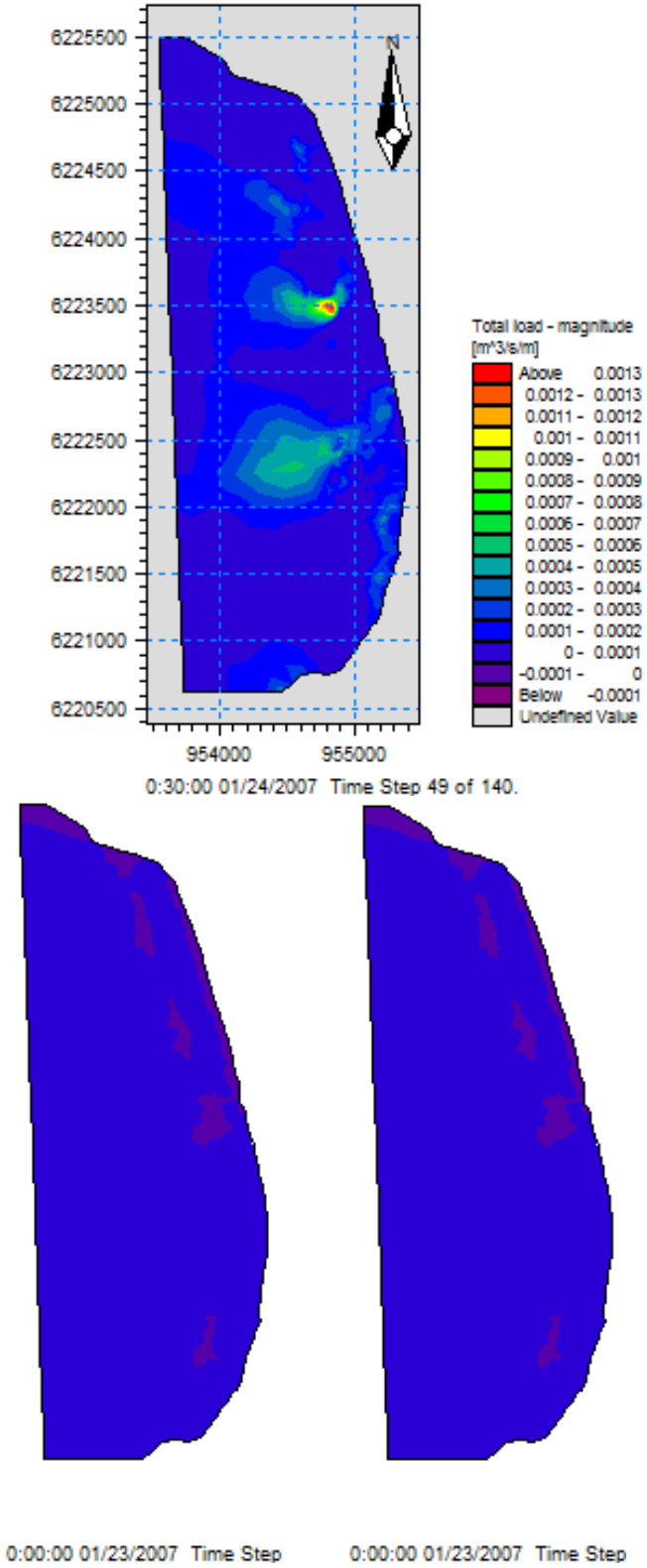

Fig. 13 Maps of the sediment transport (same color palette) at the peak of the western storm (upper), Mistral storm (lower, left), and southwestern storms (lower, right)

1) North Zone

It spreads from north boundary to B03 (Fig. 10). During the western storms, the wave model indicates strong swells focus

between the north boundary and B03 landmarks (Fig. 11). The highest was 1.6m in the direction 236°. Rip currents can reach 0.33 m/s and 122° (Fig. 12), resulting in a complex sediment transport in the channel between north boundary to B03 with low erosion (-0.0039 m/day), focused on B01 and B03 (Fig. 13). Sediment transport is characterized by the south-north direction at an average rate of $18.9.10^{-7}$ $m^3/s/lm$ (59.6 m^3/year/linear meter of coast). At the landmark B01, the maximum wave energy density can reach 1.47 $m^2/s/rad$.

During episodes of Mistral, the wave model indicates strong swells focus between north boundary and B03 landmarks. The highest was 1.7m in the direction 216° to 264°. Rip currents can reach 0.33 m/s and 120°, erosion reaches -0.004 m/day, focused on B01 and B03. Sediment transport is characterized by the south-north direction at an average rate of 20.10^{-7} $m^3/s/lm$ (63 m^3/year/linear meter of coast). At the landmark B01, the maximum wave energy density can reach 1.61 $m^2/s/rad$.

During southwestern storms, rip current speeds can reach 0.67 m/s northwestern direction. Swell direction varies 170° to 180°, is strong, around 2.2m. The morphological changes indicate sediment deposits in this zone. Strongest erosion reaches 0.0023 m/day. At the landmark B01, the maximum wave energy density can reach 1.49 $m^2/s/rad$.

In north zone, the maximum wave energy density corresponds to frequency 0.119 Hz (wave period 8.4 s) at the landmark B01.

2) North-Central Zone

It spreads from landmark B03 to B16 (Fig. 10). During the western storms, the wave model indicates strong swells focus between B03 and B16 landmarks. The highest was 1.8m in the direction 253°. The longitudinal currents can reach 0.7 m/s to the north. Rip currents can reach 0.67 m/s and 167 °, resulting in a complex sediment transport in the channel between landmarks B03 and B16 with low erosion (-0.0072 m/day), focused on B03 and B10. Sediment transport is characterized by the South-North direction at an average rate of 273.10^{-7} $m^3/s/lm$ (861 m^3/year/linear meter of coast).

During episodes of Mistral, the model reproduces the swell direction of 216 ° to 264 ° of low average height 1.9m. Rip currents can reach 0.68 m/s. The longitudinal current is north-south in direction. The maximum erosion is of -0.008 m/day. Sediment transport to the South reached 280.10^{-7} $m^3/s/m$ (883 m^3/year/lm).

During southwestern storms, rip current speeds can reach 0.67 m/s northwestern direction. Swell direction varies 190° to 200°, is strong, around 1.9m. The morphological changes indicate widespread erosion from B03 to B08, and concentrated sediment deposits in the central zone. Strongest erosion reaches 0.007 m/day, transportation reached 283.10^{-7} $m^3/s/m$ (892 m^3/year/lm) to the north.

Fig. 14 represents in red the maximal wave spectral value, which corresponds to the energy pic value (E). This pictures the most visible waves. They come from sector West-South-West at period 8.4s. Wave spread is relatively small, and waves present long ridges.

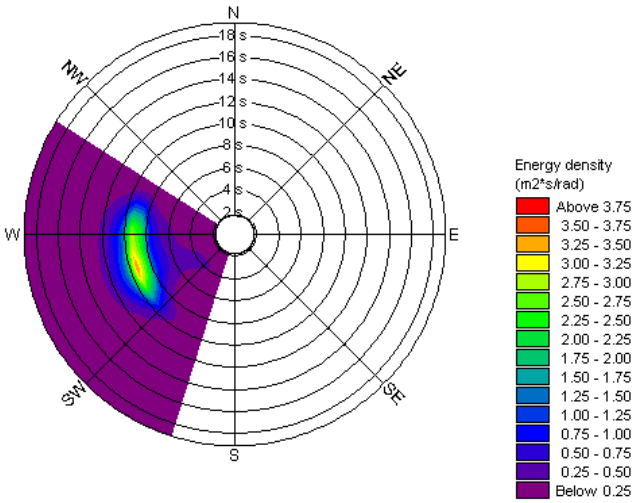

Fig. 14 Simulated directional spectra at the peak of the southwestern storms at the landmark B08

The maximum wave energy density has also been extracted on shore for the different landmarks B04, B06, B08, B10, B13, and B16. The results are collected in the Table III:

TABLE III
THE MAXIMUM WAVE ENERGY DENSITY IN NORTH-CENTRAL ZONE

LM	Southwestern storms			Western storms			Mistral storms		
	E	f	T	E	f	T	E	f	T
B04	3.30	0.116	8.6	3.44	0.119	8.4	3.60	0.119	8.4
B06	3.10	0.108	9.3	2.86	0.116	8.6	3.00	0.116	8.6
B08	2.90	0.108	9.3	2.56	0.116	8.6	2.65	0.116	8.6
B10	2.80	0.108	9.3	2.42	0.116	8.6	2.44	0.116	8.6
B13	3.80	0.108	9.3	3.33	0.116	8.6	3.42	0.116	8.6
B16	3.50	0.108	9.3	2.9	0.108	9.3	3.07	0.108	9.3
B17	3.90	0.108	9.3	3.13	0.116	8.6	3.32	0.108	9.3
B18	2.65	0.108	9.3	2.38	0.116	8.6	2.38	0.108	9.3
B23	1.20	0.116	8.6	1.36	0.116	8.6	1.35	0.116	8.6
B33	0.85	0.119	8.4	0.87	0.119	8.4	1.01	0.119	8.4
B41	0.35	0.131	7.7	0.42	0.131	7.7	0.49	0.131	7.7

LM = landmarks; E = wave energy density, $m^2/s/rad$;
f = frequency, Hz; T = period, s.

3) Central Zone

It is from landmark B16 to B23 (Fig. 10). By western storms, the model reproduces swell 261° direction, of height 1.5m. Rip currents go 167° at the speed of 0.67 m/s. Erosion rate on the average is -0.011 m/day.

During mistral episodes, rip currents are 0.67 m/s too, swell is direction 264° to 280° of low height 1.6m. Erosion is lower at -0.012 m/day.

During southwestern tempests, rip currents are close to 0.67 m/s with waves pointing to 200° to 210° of height 1.4m. Erosion speed goes up to 0.004 m/day, sediment transport, northern, reaches 350.10^{-7} $m^3/s/lm$ (1103 m^3/year/lm).

The maximum wave energy density has also been extracted on shore for the different landmarks B17, B18, and B23. The results are collected in the Table III.

4) Southern Zone

It is from landmark B23 to B46 (Fig. 10). During western storms, the model shows wave heights rarely exceed 1.5 m, 261° in direction. Sagittal 186° steering currents are weak, around 0.68 m/s. Erosion reached 0.008 m/day, corresponding to a sediment transport of 376 10^{-7} m^3/s/lm north.

During episodes of Mistral rip currents are close to 0.68 m/s. The swell direction is 220° to 270° heights around 1.5m. But the erosion rate is around 0.008 m/day. Sediment transportation is low, 380.10^{-7} m^3/s/lm south (1198 m^3/year/lm).

During southwestern storms, rip currents reach 0.68 m/s. The wave heights are significant 1.3m (direction 200° to 220°). Erosion modeled is around 0.003 m/day, sediment transport to the south coast at 386.10^{-7} m^3/s/lm north.

The maximum wave energy density has also been extracted on shore for the different landmarks B33, and B41. The results are collected in the Table III.

IV. Conclusion

Preliminary simulations that have been satisfactorily calibrated on real data have driven to the identification of spatio-temporal differences of the hydro-sedimentologic dynamics of the area of study. This has led us to subdivide the area into four cells: northern, northern-central, central and southern.

Southwestern storms generate the higher waves (2.2 m) and higher energy density (3.9m^2/s/rad) compared to western ones or mistral episodes. Onshore, waves arise in areas exposed to South-Western directional waves, which present a small spread and long ridges.

Rip currents play an important role in the sediment transport during storms. Erosion never vanishes in the northern zone between landmarks B03 and B08, maximal during southwestern storms, while central and southern zones present accretion phenomena and week erosion.

These results are to be interpreted carefully, regarding the little amount of available data for the calibration process. However with so little data we recover the approximate dynamic's behavior as described in earlier studies.

Therefor the main conclusion is that our approach for the model deserves finer development, in order to estimate the effect of coast protecting constructions on the gulf of Giens. This is the subject of a forthcoming paper.

Acknowledgment

We would like to thank the following organizations who have kindly provided data possible: SHOM, EMODnet, IGN, CETMEF, EOL, IFREMER, ECMWF, and GIS Posidonie.

References

[1] J. J. Blanc, "Etude sédimentologique de la presqu'île de Giens et de ses abords," Rapport final,1960.

[2] A. Falsan, "Carte géologique et minéralogique des environs d'Hyères," ed. Lyon: imp. de G. Marmorat, 1863.

[3] L. Léger and Blanchet, "Sur l'existence de plages fossiles aux îles d'Hyères," Laboratoire de Pisciculture, Grenoble, Travaux du laboratoire de Pisciculture, Grenoble,1927.

[4] H. Parent, "Le cours du Gapeau a travers les âges," *La Vie Hyèroise,* pp. 7-8, 1924.

[5] J. J. Blanc, "Recherches sédimentologiques sur la protection du littoral à la presqu'ile de Giens (Var)," Rapport final,1973.

[6] A. Jeudy De Grissac, "Sédimentologie dynamique des rades d'Hyères et de Giens (Var). Problèmes d'Aménagements," Ph.D. dissertation, Université d'Aix-Marseille II, Marseille, 1975.

[7] J. Courtaud, "Dynamiques géomorphologiques et risques littoraux cas du tombolo de Giens (Var, France méridionale)," Ph.D. dissertation, Université Aix-Marseille I, 2000.

[8] ERAMM, "Etude sur la protection de la partie Nord du tombolo Ouest de Giens," Rapport final,2001.

[9] IARE, "Le Tombolo Occidental de Giens - Synthèse des connaissances- Analyse globale et scenarios d'aménagement et de gestion," Rapport final,1996.

[10] P. Serantoni and O. Lizaud, "Suivi de l'évolution des plages de la commune Hyères-les-palmiers," Rapport final,2000-2010.

[11] SOGREAH, "Défense du littoral oriental du golfe de Giens," Rapport final,1988.

[12] SOGREAH, "Protection du tombolo Ouest," Rapport final,1988.

[13] J. J. Blanc, "Phénomènes d'érosions sous-marines à la Presqu'île de Giens (Var)," *CR Acad. Sci. Paris,* vol. 278, pp. 1821-1823, 1974.

[14] P. Farnole, J. Bougis, M. Ritondale, and M. Barbarroux, "Protection du littoral contre l'érosion marine: application au tombolo Ouest de Giens," in *VIIèmes Journées Nationales Génie Civil- Génie Côtier*, Anglet, France, 2002, pp. 513-522.

[15] DDE and CETE, "Protection du Tombolo Ouest de Giens. Etude de dune," Hyères, Rapport final,1992.

[16] HYDRO M, "Etude d'impact sur l'environnement du projet de protection du tombolo ouest de la presqu'ile de Giens," Rapport final,1993.

[17] M. Luhar, S. Coutu, E. Infantes, S. Fox, and H. Nepf, "Wave-induced velocities inside a model seagrass bed," *Journal of Geophysical Research: Oceans (1978–2012),* vol. 115, 2010.

[18] M. Nieri, P. Francour, S. Sartoretto, O. Sloeck, and F. Urscheller, "Cartographie des peuplements benthiques, des types de fond et de l'herbier de posidonies autour du port Saint-Pierre-d'Hyères," Marseille, Rapport final,1992.

[19] H. M. Nepf, C. G. Mugnier, and R. A. Zavistoski, "The effects of vegetation on longitudinal dispersion," *Estuarine, Coastal and Shelf Science,* vol. 44, pp. 675-684, 1997.

[20] T. Koftis and P. Prinos, "Estimation of wave attenuation over Posidonia oceanica," in *5th SCACR International Short Conference on Applied Coastal Research: proceedings*, RWTH Aachen University, Germany. Mitteilungen des Lehrstuhls und Instituts für Wasserbau und Wasserwirtschaft de, 2011, pp. 264-271.

[21] S.-N. Chen, L. P. Sanford, E. W. Koch, F. Shi, and E. W. North, "A nearshore model to investigate the effects of seagrass bed geometry on wave attenuation and suspended sediment transport," *Estuaries and Coasts,* vol. 30, pp. 296-310, 2007.

[22] DHI, "MIKE 21 Spectral Wave Module Scientific Documentation," 2014.

[23] DHI, "MIKE 21 & MIKE 3 FLOW MODEL FM - Hydrodynamic and Transport Module - Scientific Documentation," 2014.

[24] DHI, "MIKE 21 ST - Non-Cohesive Sediment Transport Module - User Guide," 2014.

[25] DHI, "MIKE 21/3 Couple Model FM," 2014.

[26] M. Uddin, J. B. Alam, Z. H. Khan, G. M. J. Hasan, and T. Rahman, "Two Dimensional Hydrodynamic Modelling of Northern Bay of Bengal Coastal Waters," pp. 12-12, 2014.

[27] ERAMM, "Etude de faisabilité courantologie et sédimentologique préalable au projet d"extension du port des Oursinières," Rapport final,2000.

[28] S. Meulé, "IMplantation d'Atténuateur de Houle en GEOtextile: Suivi scientifique de la plage de La Capte, Hyères, Var : Instrumentation, Modélisation," Hyères, Rapport final,2010.

[29] L. C. v. Rijn, D. J. R. Walstra, B. Grasmeijer, J. Sutherland, S. Pan, J. P. Sierra*, et al.*, "The predictability of cross-shore bed evolution of sandy beaches at the time scale of storms and seasons using process-based profile models," *Coastal Engineering,* vol. 47, pp. 295-327, 2003.